Rahman, Md Habibur and Li, Rui and Yao, Liangzhong and Xu, Lie (2018) Protection and post-fault recovery of large HVDC networks using partitioning and fast acting DC breakers at strategic locations. In: The 14th IET International Conference-AC and DC Power Transmission (ACDC 2018). IET, Stevenage, pp. 1-8. (In Press) ,

Protection and Post-Fault Recovery of Large HVDC Networks Using Partitioning and Fast Acting DC Breakers at Strategic Locations

Md Habibur Rahman [1*], Rui Li[1], Liangzhong Yao[2], Lie Xu [1]

[1] Department of Electronic & Electrical Engineering, University of Strathclyde, Glasgow, UK
[2] China Electric Power Research Institute, Xiaoying Road, Beijing, 100192, China
[*]habibur.rahman@strath.ac.uk

Keywords: Network Partitioning, DC Fault, DC Circuit Breakers, Fault Protection, Post-fault Recovery

Abstract DC fault protection arrangements for a large multi-terminal HVDC network are proposed where fast-acting DC circuit breakers are only used at strategic locations with the large DC network to be operated interconnected but partitioned into islanded DC zones in case of any DC fault events in one of the DC zones. Each DC network zone can be protected using low cost, slow protection devices such as AC circuit breakers coordinated with DC switches or slow mechanical type DC circuit breakers. This ensures the maximum 'loss-of-infeed' for any AC networks connected to the large HVDC system is kept within acceptable limits with reduced investment in protection cost as expensive fast acting DC circuit breakers are kept to a minimum. A post-fault recovery method of the faulty section is proposed including the reconnection with the healthy part of the network to ensure reliable and smooth restoration of the large multi-terminal HVDC network. A detailed pre-fault and post-fault power flow analysis is also conducted in a multi-terminal DC network with DC voltage droop control. The proposed protection arrangements and post-fault recovery method are validated by simulation of a two-zone, six-terminal DC network with respective radial and meshed configurations.

1. Introduction

A DC fault event in a multi-terminal HVDC (MTDC) network brings significant protection challenges due to the low impedance of the DC network resulting in step rise in fault current and fast DC voltage collapse. This may cause serious damage to the converters and potential disruption in power flow across the entire network or even leading to complete shutdown of the whole MTDC network for a prolonged period [1]. Therefore, a robust and accurate protection arrangement is required to identify the fault and its location and isolate the faulty segment in a selective manner so as to enable fast restoration of the MTDC network.

Many protection strategies for MTDC network have been studied and analysed [1-4]. In [1] a 'handshaking' method was proposed to protect VSC based MTDC network where DC switches (DC disconnectors) and AC circuit breakers (ACCBs) are used. This approach is one of the economical protection arrangements compared to others but it leads to complete shutdown of the entire network before the faulty section is isolated and the system post-fault recovery process is prolonged. Therefore, the proposed concept can pose major operational problems for a large MTDC network due to the unacceptable large 'loss-of-infeed' connected to an AC network [5]. Another concept has been proposed in [2] where mechanical DC circuit breakers (DCCBs) with additional DC passive components (DC reactor and capacitor) and active converter control are used to reduce DC fault current. This proposed concept, however, leads to some additional cost as well as increased system footprint for a large MTDC network. In [3] a low-speed protection method has been considered to protect DC transmission grid using slow mechanical DCCBs (SDCCBs) and fault tolerant LCL voltage source converter.

To protect a large MTDC network in case of any DC fault events there are two possible ways that have been studied in literature without causing large 'loss-of-infeed'. The first option is to equip DCCBs at each end of DC cables in the MTDC network which can quickly isolate the faulty section without interrupting the rest of the network. Various types of DCCBs have been proposed [6-8] for DC network protection, such as solid-state DCCBs, hybrid DCCBs and mechanical type DCCBs. DCCBs like solid state and hybrid types are capable of operating within a few milliseconds but incur excessively high capital cost and large footprint which incurs further cost if, as for an application that connects offshore wind farms, required to be installed on an offshore platform. In contrast, mechanical type DCCBs have low capital cost and power loses [3]. A second option is to use converter topologies with DC fault blocking capability. Full-bridge based modular multilevel converters (MMCs) are capable of blocking the DC fault current but use additional semiconductor devices leading to higher capital cost and power loss compared to the half-bridge MMC [9, 10]. In addition, such converters usually can protect themselves from over-current but the large MTDC network has to be shut down and additional DC protection equipment is still required to isolate the faulty section.

This study mainly focuses on a DC fault protection arrangement and system recovery strategy of a large partitioned multi-zone MTDC network where fast-acting DCCBs are only installed at strategic locations to allow quicker fault isolation of faulty zones with reduced capital cost and power losses. The main purpose of the protection arrangement is to minimize the use of expensive DCCBs while ensuring the maximum 'loss-of-infeed' is within operation limit. A post-fault system recovery strategy, which significantly reduces the DC voltage overshoot compared to conventional ones so as to reduce the voltage stress of the DC side components, is proposed and studied.

The rest of the paper is structured as follows. Section 2 describes the concept of MTDC network partition and the system configuration. System protection and recovery strategies are outlined in Section 3. A detailed system pre-fault and post-fault power flow analysis is conducted in Section 4. In Section 5, a case study in Matlab/Simulink environment is performed to demonstrate the validity of the proposed protection arrangement and post-fault recovery and, finally, Section 6 draws the conclusions.

2. DC Network Partition and Configuration

2.1. DC Network Partitioning

The largest permanent 'loss-of-infeed' for which the system operator for the transmission system in Great Britain (GB) should ensure stability is 1.8 GW [11]. The maximum temporary 'loss-of-infeed' could potentially be higher though it will be dependent on the fault type, duration etc. For a future large-scale MTDC system, to ensure the maximum 'loss-of-infeed' is not exceeded for a single DC fault, significant challenges need to be overcome.

In order to limit the impact of a fault, one possible solution is to install fast acting DCCBs at every DC cable connection point but such an arrangement incurs a huge cost in system protection. Therefore, a number of facts need to be considered while configuring a large MTDC network protection such as the infrequency of DC fault events, relatively low loading factor of power generation from wind farms and the investment in system protection. To rationalize the cost and reliable system operation, partitioning a large MTDC network into a number of small DC network zones can be an option where each DC network zone is configured in such a way that the total 'loss-of-infeed' is kept below the maximum acceptable power loss for the connected AC network [5, 12].

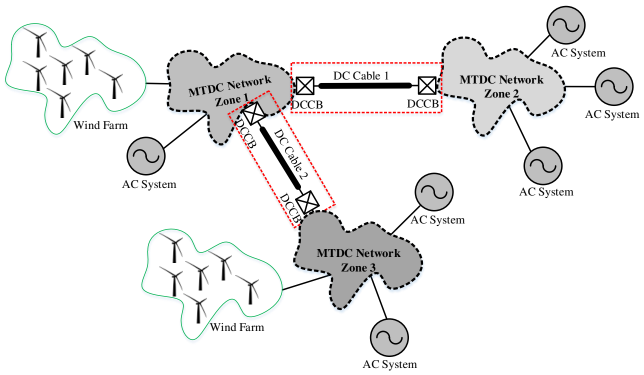

Fig. 1. Partitioned large MTDC networks using fast-acting DCCBs at strategic locations

In case of a fault event in a particular zone, the fault can be isolated and cleared by ACCBs and DC switches [1]. However, network partitioning reduces the operational flexibility of the MTDC network. An alternative option for protecting a large MTDC network is to use fast acting DCCBs located at strategic locations, joining different DC network zones and allowing the entire network to be operated interconnected in the pre-fault condition but partitioned into islanded DC network zones following any fault events. An example of a large MTDC network configuration is shown in Fig.1 where fast-acting DCCBs are used at strategic locations, i.e. each end of Cables 1 and 2. In case of a fault event in one of the DC network zones the other two DC network zones can remain operational by opening the fast acting DCCBs on the cable connecting to the faulty DC zone. Within each DC network zone, different protection arrangements can be used, e.g. slow mechanical DCCBs or ACCBs with DC switches, depending on its network configuration and operation requirement.

2.2. System Configuration

Fig.2 shows the six-terminal MTDC system considered in the paper consisting of six half-bridge MMC based converters connected to six AC systems. The system contains two DC network zones which are interconnected by DC cables (C14) equipped with fast-acting DCCBs (FDCCB 14 and 41). To reduce the cost, no fast acting DCCBs are used inside either of the two DC network zones.

The meshed network configuration in DC network Zone 1 has increased service reliability due to redundant supply channels and slow mechanical DCCBs are installed to achieve the maximum benefit of its configuration. The 3-terminal radial DC network Zone 2 is protected using ACCBs and DC switches which is a slow but low-cost protection arrangement.

Average value MMC models are used in this study [13]. In the simulations, π models of the DC cables are considered. DC inductors of 100mH are added to MMC DC terminals to reduce the rate of rise of the fault current and to provide an additional time to deal with protection decision [14].

3. System Protection and Recovery

3.1. System Protection

The main objective for the DC partitioning is to keep the healthy zones in a large MTDC system operational all times following a DC fault by means of using fast-acting DCCBs at strategic locations to isolate the faulty zone, such that the maximum loss-of-supply is not exceeded. The following protection arrangements are considered for the proposed system to isolate a DC fault and allow the healthy zones to remain operational.

3.1.1. Protection for DC Network Zone 1 (Meshed Network)

In this study, Zone 1 is protected using slow mechanical DCCBs. During a fault event in Zone 1, all converters in the faulty zone will experience high over-current and therefore, the converters are blocked immediately once the converter arm currents reach the predefined threshold value ($I_{arm} > 2\,p.u.$).

Fig. 3(a) illustrates DCCB protection technique where the green arrows indicate pre-fault DC current direction and the red arrows (dotted) indicate current direction during the fault at cable C45. If the locally measured DC fault current at a DCCB goes above the predetermined set value ($I_{dc} > 2\,p.u.$) and the detected over-currents flow into the DC cables, the DCCB will be opened (with a 20ms delay for slow

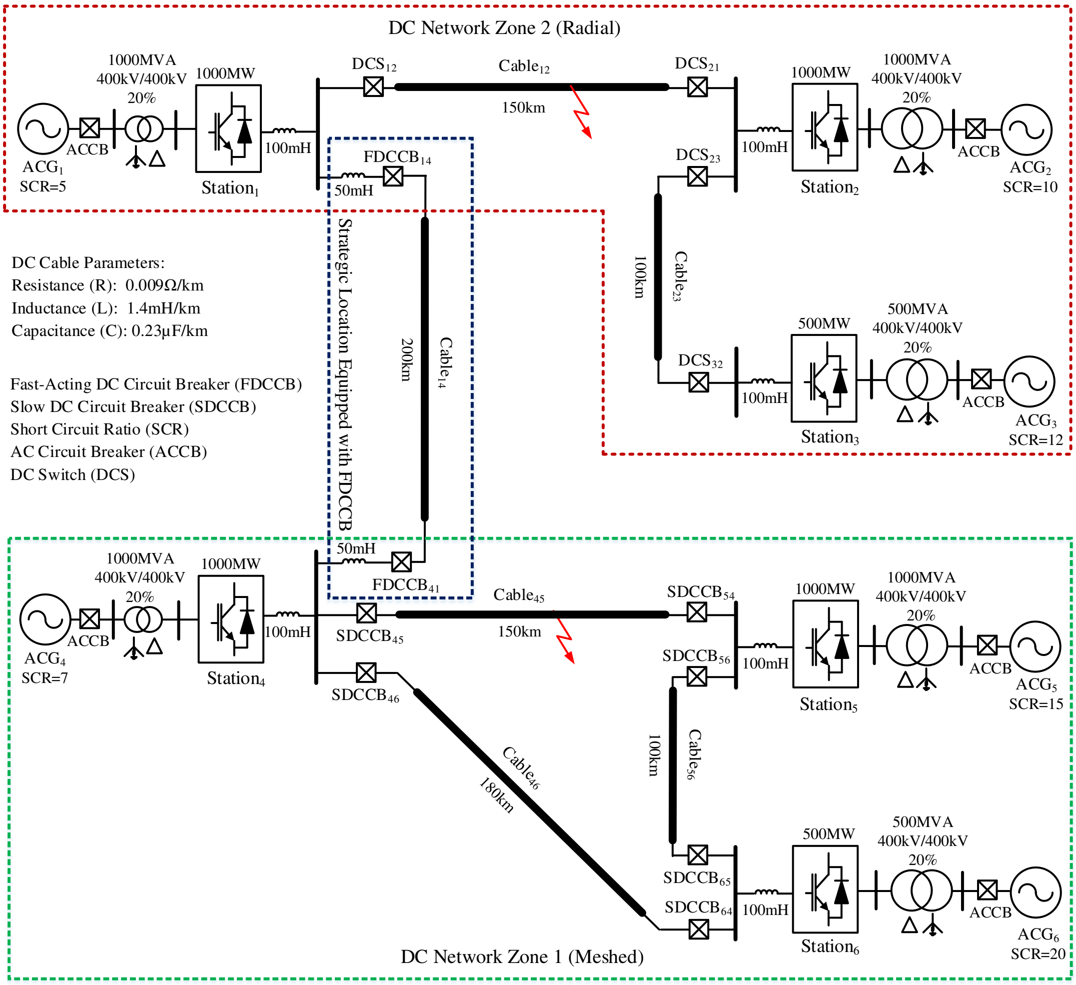

Fig. 2. Block diagram of a six terminal MMC based MTDC network

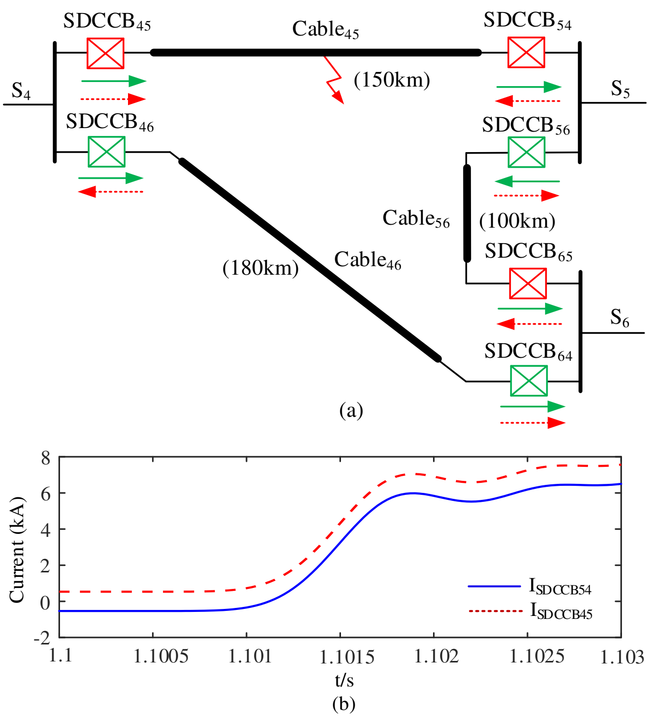

Fig. 3. DCB protection technique and current flowing through DC circuit breaker in faulty cable where a line-to-line fault is applied at the midpoint of cable C45 at 1.1s

(a) DCCB protection technique, (b) current flowing through SDCCB45 and SDCCB54
mechanical DCCB[15] in this study). With a DC line-to-line fault applied at cable C45 as shown in Fig.3(a), both ends of the faulty cable (C45) will see current flowing towards the fault leading to the opening of the DCCBs at both ends of C45 (SDCCB 45 and 54).

For other cables only DCCBs at one side of each cable may see fault current flowing into the cable, e.g. SDCCB65 at cable C56. For the two ends of cable C46, depending on the fault location at C45 and the relative cable lengths, the detected over-currents at SDCCB 46 and 64 may both flow out from the DC cable (as the example shown in Fig.3(a)) and therefore, both SDCCB 46 and 64 will remain closed. Alternatively, one end of cable C46 may see current flowing into the cable leading to the trip of one SDCCB connected to C46 (this scenario not shown in Fig. 3(a)).

Fig. 3(b) shows an example of the DC current at SDCCB45 and SDCCB54 of cable C45. In this study, DC current flowing into a DC cable (i.e. away from the converter) is defined as positive. As can be seen from Fig. 3(b), during pre-fault condition same current flows through SDCCB45 and SDCCB54 (opposite direction) but once a line-to-line fault is applied at the midpoint of cable C45 at 1.1s, the current direction of SDCCB54 is changed and over-currents flow into the DC cable at both ends. This leads to the opening of both DCCB 45 and 54 at the two ends of the faulty cable C45.

3.1.2. Protection for DC Network Zone 2 (Radial Network)

In this radial network zone, slow mechanical DCCBs are not used due to its network configuration, system power rating and cost reduction consideration. DC protection is thus achieved by the combination of DC switches, which are installed at each end of the DC cables, and AC circuit breakers. Without FDCCBs or SDCCBs, the converters' anti-parallel diodes must be rated sufficiently for the current that flows during faults on a DC network. By-pass devices, typically thyristor, can be used to prevent damage to converter components [13]. In case of a DC fault in Zone 2, all converters will be blocked once the converter arm currents reach the pre-defined protective threshold value ($I_{arm} > 2\,p.u.$). As DC switches are not capable of interrupting DC fault currents, the break of the fault current has to be carried out by opening the ACCBs connected to all converter stations. The disconnection of all the AC sources from the DC network zone allows DC fault currents to decay. However, it may take a considerable time (in the order of 800ms-1200ms) for the DC fault current to decay to zero due to DC side inductor/capacitor and low DC cable resistance.

Similar to the DCCBs in Zone 1, only those DC switches in the faulty zone will be opened whose detected over-currents flow into the DC cables, i.e. only DCS12, DCS21 and DCS32 will trip for a DC fault applied at cable C12 as shown in Fig.2. As have been described, the DC switches can only trip when the respective DC currents reach approximately zero.

3.1.3. Strategic Location Equipped with FDCCB

This strategic location is the key part of the large MTDC network where two DC zones are interconnected. The fast-acting DCCBs are equipped at both ends of the DC cable C14 to join the two DC zones together but also provide a means to quickly isolate the faulty zone and allow the healthy part of the network to remain operational. An additional inductor (in this example, 50mH) can be installed at both ends of the cable to reduce the rate of rise of fault current and allow extra time (a few ms) to protect the healthy zone of the network [14]. In this system configuration, if the locally measured DC fault current at an FDCCB terminal goes above the predetermined set value ($I_{dc} > 2\,p.u.$) and flow into the DC cable, the FDCCB will be opened with a 3ms delay for this study [6, 7]. Thus, in the event of a fault inside one of the two DC zones, one end of the FDCCBs will activate very quick to disconnect the faulty zone from the healthy one such that the operation of the healthy zone can continue.

3.2. Post-Fault System Recovery

Post-fault system recovery process is one of the key considerations for a large MTDC system. Loss of a transmission cable due to a fault results in a reduction of overall power transmission capacity in the MTDC network which affects the remaining healthy lines of the network. Proper power rescheduling may be required to ensure stable system operation after fault, as will be discussed in Section 4. After isolating the faulty cable within the faulty zone, the remaining part of the network can be restarted and can be reconnected to the other healthy zone depending on the fault location and operation requirement. Different post-fault recovery methods have been studied in the literature [1, 16]. In [1] a 'handshaking' method was proposed to recover a system after isolating the fault where all converters are unblocked for initial a 40ms to balance the DC voltage and then blocked again before reclosing the DCCBs/DCSs to minimise the DC voltage mismatch on the two sides of the DCCBs/DCSs. Once all relevant DCCBs/DCs are reclosed, all converters are enabled to transmit power again. However, the DC voltage mismatch exists during restoration process leading to significant voltage overshoots and oscillations. Therefore, a post-fault recovery method is proposed to ensure stable and smooth system restoration with reduced DC voltage overshoot and oscillation.

3.2.1. Post-Fault Recovery for DC Fault in Zone 1

The opened SDCCBs which are not connected to the faulty cable are required to reclose before power transmission can be restarted. The following steps are considered for post-fault recovery of Zone1:

- All converter stations can be restarted (as the faulty branch has been isolated) and their operation modes are initially all set to control DC voltage.
- For an un-faulty DC cable, at least one end of the SDCCB is still closed and thus the DC cable voltages will eventually reach to their pre-set value ($V_{dc} \geq 0.95\,\mathrm{p.u.}$). For the example shown in Fig. 3, during a fault at C45, SDCCB 45, 54, and 65 are opened but the DC voltages at cable C46 and C56 recover after restarting the converters. Therefore, SDCCB65 (connecting to cable C56) is determined as not being connected to a faulty branch and can be reclosed.
- After the completion of the reclosing process, converter control modes are changed according to system operator requirements to ensure stable operation and start transmitting power.

3.2.2. Post-Fault Recovery for DC Fault in Zone 2

After isolating the faulty cable by using DC switches, the remaining part of the DC network Zone 2 is restarted. The following steps are considered for post-fault recovery of the DC network Zone 2:

- All opened ACCBs are reclosed first. The healthy cables that are still connected to the converters in Zone 2 will also be recharged. Due to the limited DC cable capacitance the inrush current is likely to be limited during this process. An alternative way is to recharge the DC cables using the energy stored in the MMC's submodule (SM) capacitors before reclosing the ACCBs [17].
- Similar to the recovery strategy for Zone 1, all converter stations are then restarted and are initially all set at DC voltage control mode.
- The DCSs are reclosed only when the DC voltages at the relevant DC cables they connected to reach their pre-set values ($V_{dc} \geq 0.95\,\mathrm{p.u.}$). For the example shown in Fig. 2, during a fault at C12, DCS 12, 21, and 32 are initially opened but the DC voltage at cable C23 recovers after restarting Station 2. Therefore, DCS32 (connecting to cable C23) is determined as not being connected to a faulty branch and can be reclosed (but not DCS 12 and 21 as cable C12 remains at low DC voltage).
- After the completion of the reclosing process, converter control modes can be changed accordingly to start transmitting power.

3.2.3. Post-Fault Fast Acting DCCB Re-Closing Stage

Fast acting DCCBs can be reclosed once the remaining part of the faulty zone is recovered and restarted fully. For a fault event in any DC network (apart from cable C14), only one FDCCB is initially opened (only one end can see fault current flowing into the DC cable) and required to reclose. Thus the healthy zone can be reconnected with the recovered DC zone.

In the proposed post-fault recovery strategy, the converter stations are all re-enabled first and operated at DC voltage control mode before reclosing the relevant DCCBs/DCSs. This provides better DC voltage control during the reclosing stage leading to less voltage oscillation and quick system recovery. In this subsection the effectiveness of this method is compared with one of the recovery method [1] which has been discussed in section 3.2. Here only one fault case scenario is considered for ease of the comparison.

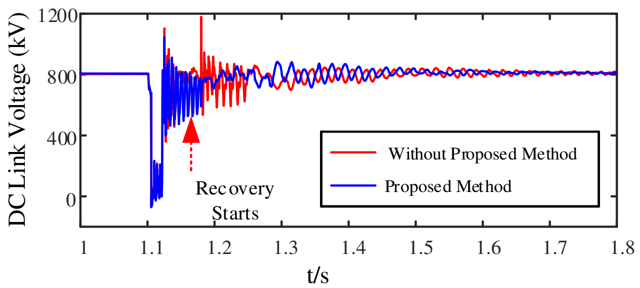

Fig. 4. Comparison between different recovery methods (Station 4)

A DC line-to-line fault is applied at the midpoint of the transmission cable C45 in DC network Zone 1 at 1.1s. Once the faulty cable is isolated from the meshed network by opening the relevant SDCCBs (45 and 54), the DC voltage recovers and the system can be restarted to resume normal operation. Fig. 4 shows the DC link voltage of Station 4 during system recovery stages which clearly indicates a smoother system recovery with reduced DC voltage oscillation for the proposed method compared to the other approach where there are significant voltage overshoot (almost 1.5p.u) and voltage oscillation. In the proposed method enabling all converters in DC voltage control mode minimizes the DC voltage differences between the different sections of the DC network (as some DCCBs/DCSs have been tripped) and consequently reduces the transients when the relevant DCCBs/DCSs are reclosed.

4. System Pre-Fault and Post-Fault Power Flow Analysis

Active power flow has to be balanced in an MTDC network, with the indicator of DC link voltage maintained within a predefined level with acceptable variation under all conditions. For a large MTDC network, it is worthwhile to have a number of stations to control the DC voltage to provide better operational flexibility of the network.

Fig. 5 shows a simplified steady-state DC network equivalent circuit of the six-terminal MTDC network presented in Fig.2. In Fig. 5, R_1 - R_6 represent the equivalent DC cable resistances of the six connection cables, V_{dc1}- V_{dc6} and I_{dc1}- I_{dc6} are the respective DC voltages and currents of the six stations at their HVDC cable connection points where (V_{dc1}, V_{dc4}) and $(V_{dc2}, V_{dc3}, V_{dc5}, V_{dc6})$ are the sending end and receiving end voltages respectively.

4.1. Power Flow Analysis

In the HVDC network shown in Fig. 2, Stations 1, 3, 4 and 6 are set for controlling the active power of the network whereas Stations 2 and 5 are set to control the DC link voltage of the entire network with a PI regulator and droop control respectively. Thus, under steady-state, the DC voltage at Station 2 can be considered to be the nominal DC voltage (PI controller gives zero steady-state error) and the DC current at Station 5 is given as $I_{dc5} = K_5(V_{dc5} - V_{dc5}^*)$. Taking I_{dc1}, $V_{dc2}, I_{dc3}, I_{dc4}, V_{dc5}^*$ and I_{dc6} as the inputs of the six-terminal network, the pre-fault network power flow is given by matrix in (1).

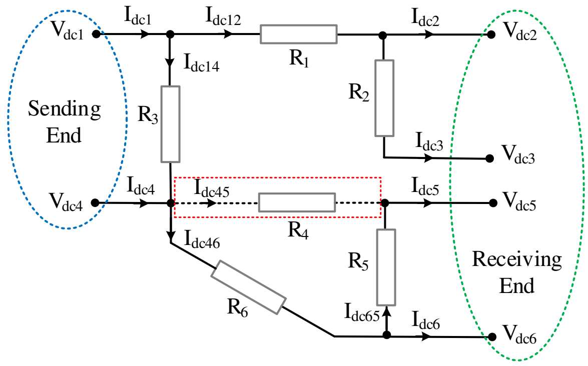

Fig. 5. Steady-state DC equivalent circuit for the six-terminal MTDC network

A similar approach is applied for post-fault power flow analysis, considering cable C45 is isolated from the network and all system control modes are restored to the pre-fault state after system recovery. An alternative method is to consider R_4 in (1) to be infinite due to the disconnection of cable C45. Thus, the post-fault power flow can be calculated using the same matrix in (1) by considering $R_4=\infty$.

4.2. System Pre-Fault and Post-Fault Power Flow Analysis Result

The six-terminal network shown in Fig.2 is simulated in MATLAB/SIMULINK environment to validate the simplified mathematical representation presented in (1). The parameters for the six-terminal MTDC system are given in Fig.2 and the nominal DC link voltage of the DC system is ±400kV. Stations 1 and 4 send 700MW and 800MW power to the DC grid, respectively while Stations 3 and 6 receive 400MW power each from the DC grid to their respective AC grids. Stations 2 (PI) and 5 (droop) regulate the DC link voltage of the entire network to ensure effective active power sharing. In this case study, all converters are operated with unity power factor.

The pre-fault and post-fault power flow analysis for both calculated and simulated results are presented in Table 1 where $V_{dc5}^* = 784$kV and $K_5 = 0.0469$ (or 30 based on per unit values of 800kV and 1000MW). The simulation results are in good agreement with the mathematical ones derived from (1). To maintain the same power flow from Zone 1 to Zone 2 after fault, the droop characteristic at Station 5 can be changed from per unit value of 30 to 40 and the calculated and simulated results are also compared in Table 1.

This paper is a post-print of a paper submitted to and accepted for publication in The 14th IET International Conference-AC and DC Power Transmission (ACDC 2018) and is subject to Institution of Engineering and Technology Copyright. The copy of record is available at IET Digital Library.

$$\begin{bmatrix} V_{dc1} \\ I_{dc2} \\ V_{dc3} \\ V_{dc4} \\ I_{dc5} \\ V_{dc6} \end{bmatrix} = \begin{bmatrix} \left[R_1 - \frac{R_1{}^2}{\alpha}\right] & \left[1 - \frac{R_1}{\alpha}\right] & 0 & \left[R_1 - \frac{R_1\delta}{\alpha}\right] & \frac{R_1}{\alpha} & -\left[R_1 - \frac{R_1\gamma}{\alpha}\right] \\ \left[1 - \frac{R_1}{\alpha}\right] & -\frac{1}{\alpha} & -1 & \left[1 - \frac{\delta}{\alpha}\right] & \frac{1}{\alpha} & -\left[1 - \frac{\gamma}{\alpha}\right] \\ 0 & 1 & -R_2 & 0 & 0 & 0 \\ \left[R_1 - \frac{R_1\delta}{\alpha}\right] & \left[1 - \frac{\delta}{\alpha}\right] & 0 & \left[\delta - \frac{\delta^2}{\alpha}\right] & \frac{\delta}{\alpha} & -\left[\delta - \frac{\delta\gamma}{\alpha}\right] \\ \frac{R_1}{\alpha} & \frac{1}{\alpha} & 0 & \frac{(R_1 + R_3)}{\alpha} & -\frac{1}{\alpha} & -\frac{\gamma}{\alpha} \\ \left[R_1 - \frac{R_1\beta}{\alpha}\right] & \left[1 - \frac{\beta}{\alpha}\right] & 0 & \left[\delta - \frac{\delta\beta}{\alpha}\right] & \frac{\beta}{\alpha} & -\left[\left[(\delta + R_6) - \frac{R_6{}^2}{(R_4 + R_5 + R_6)}\right] - \frac{\gamma\beta}{\alpha}\right] \end{bmatrix} \begin{bmatrix} I_{dc1} \\ V_{dc2} \\ I_{dc3} \\ I_{dc4} \\ V_{dc5}^{*} \\ I_{dc6} \end{bmatrix} \quad (1)$$

Where $\alpha = \left[\frac{1}{K_5} + \left[(R_1 + R_3) + \frac{R_4(R_5 + R_6)}{(R_4 + R_5 + R_6)}\right]\right]$, $\beta = \left[(R_1 + R_3 + R_6) - \frac{R_6(R_5 + R_6)}{(R_4 + R_5 + R_6)}\right]$,

$\gamma = \left[(R_1 + R_3) + \frac{R_4 R_6}{(R_4 + R_5 + R_6)}\right]$ and $\delta = (R_1 + R_3)$.

Table 1 System Pre-Fault and Post-Fault Power Flow Results

Voltage and Current (Station Control Mode)		**Pre-fault power flow $K_5(pu) = 30$**		**Post-fault power flow $K_5(pu) = 30$**		**Post-fault power flow $K_5(pu) = 40$**	
		Calculated	Simulated	Calculated	Simulated	Calculated	Simulated
Station 1 (P)	V_{dc1}(kV)	801.68	801.70	801.98	802.00	801.68	801.85
Station 2 (V_{dc})	I_{dc2}(A)	123.84	121.20	233.97	229.40	121.46	118.87
Station 3 (P)	V_{dc3}(kV)	799.10	799.10	799.10	799.10	799.10	799.20
Station 4 (P)	V_{dc4}(kV)	800.78	800.80	801.47	801.50	800.77	800.90
Station 5 (V_{dc})	I_{dc5}(A)	751.15	740.80	641.02	630.40	753.53	741.41
Station 6 (P)	V_{dc6}(kV)	798.99	799.00	797.78	797.80	796.70	796.80
Cable (C14)	I_{dc14}(A)	251.16	248.16	141.66	140.00	252.77	249.40

5. Simulation Results

5.1. Fault in DC Network Zone 1

As illustrated in Fig. 2, a line-to-line fault is applied at 1.1s at the midpoint of the transmission cable C45 in DC network Zone 1 (meshed network). The main concept of this protection arrangement is that, in case of any fault events within Zone 1, the fast-acting DCCBs installed at cable C14 can quickly isolate the faulty Zone 1 such that the DC network Zone 2 can remain operational.

5.2. System Behaviour during Fault

The DC link voltages, active power at the converter stations, and DC currents flowing through the DCCBs are presented in Fig.6 and Fig.7 respectively. Table 2 illustrates the sequence of events during fault isolation and system recovery where all the different stages are also indicated in Fig.6 and Fig.7 with numbers for ease of demonstration. It can be seen from Fig.6(b) that the DC voltages at Station 4-6 in Zone 1 are severely affected after fault initiation showing immediate drops with oscillation.

The DC currents measured at the DCCBs as shown in Fig.7 also shows a significant increase due to the discharge of the DC cable capacitors and fault current feeding from the converters.

Table 2 Fault Isolation and System Recovery Stages

Stage	**Event Descriptions**
①	A line-to-line fault is initiated at 1.1s at the midpoint of the transmission cable C45.
②	Station 4-6 are blocked at 1.104s, 1.106s and 1.105s respectively.
③	FDCCB 14 is opened at 1.109s while FDCCB41 remains closed.
④	SDCCB45, 54 and 65 are opened at 1.122s, 1.122s and 1.124s respectively while SDCCB46, 64, and 56 remain closed.
⑤	Station 4-6 are enabled at 1.159s, 1.161s and 1.160s, respectively.
⑥	SDCCB65 is reclosed at 1.274s.
⑦	Power of Station 4 and 6 ramp up at 1.4s.
⑧	FDCCB14 are reclosed at 1.51s to reconnect Zone 1 with healthy Zone 2.

Faults are detected in each converter located in Zone 1 using automatic arm over-current detection and blocking method in which converters are blocked once their arm currents reach the predefined set values ($I_{arm} > 2\, p.u.$). In the simulation, Station 4-6 converters are blocked 4ms, 6ms, and 5ms respectively after the fault initiation at 1.1s (see stage 2). The DC over-current flowing through the fast acting DCCBs is detected when DC fault current goes above the pre-determined set value ($I_{dc} > 2\ p.u.$) resulting the opening of the fast acting DCCBs to isolate Zone 1 from the healthy Zone 2, i.e. FDCCB14 of cable C14 is opened first.

In this simulation FDCCB14 is opened 9ms after the fault initiation (6ms fault detection time using overcurrent and 3ms opening delay time) at 1.109s (see stage 3 in Table 2). It is obvious that there is a significant power variance in Station 2 as can be seen in Fig.6(c) due to the disconnection of cable C14 from Zone 1.

The slow DCCBs are opened with 20ms mechanical delay after over-current detection and only those DCCBs whose detected over-currents flowing into the connected DC cables are opened. As the fault is applied at cable C45, DCCBs at both ends of C45 see current flowing into the fault and are opened. Therefore, C45 is isolated by SDCCB 45 and 54 as their positive over-current flowing into the cable as shown in Fig.7(c). DCCB65 at cable C56 also sees positive fault current flowing into the cable (as shown in Fig.7(d)) whereas DCCBs at both end of cable C46 see currents flowing out of the cable. Therefore, SDCCB46 and SDCCB64 remain closed. In this simulation SDCCB 45, 54 and 65 are opened after 22ms, 22ms and 24ms respectively from fault initiation (including a 20ms mechanical delay for SDCCBs) as indicated by stage 4 in Fig. 7 and Table 2.

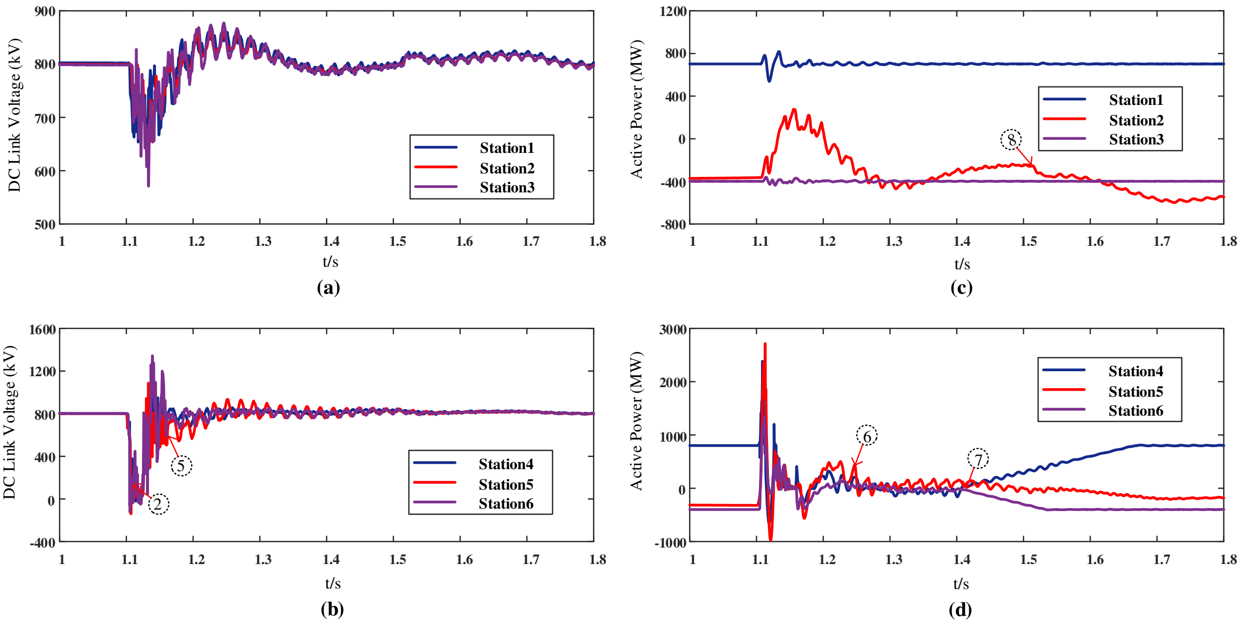

Fig. 6. System behaviour during fault isolation and restoration processes after a fault event in Zone 1 at 1.1s
(a) DC link voltage for station 1-3, (b) DC link voltage for station 4-6, (c) Active power for station 1-3, (d) Active power for station 4-6

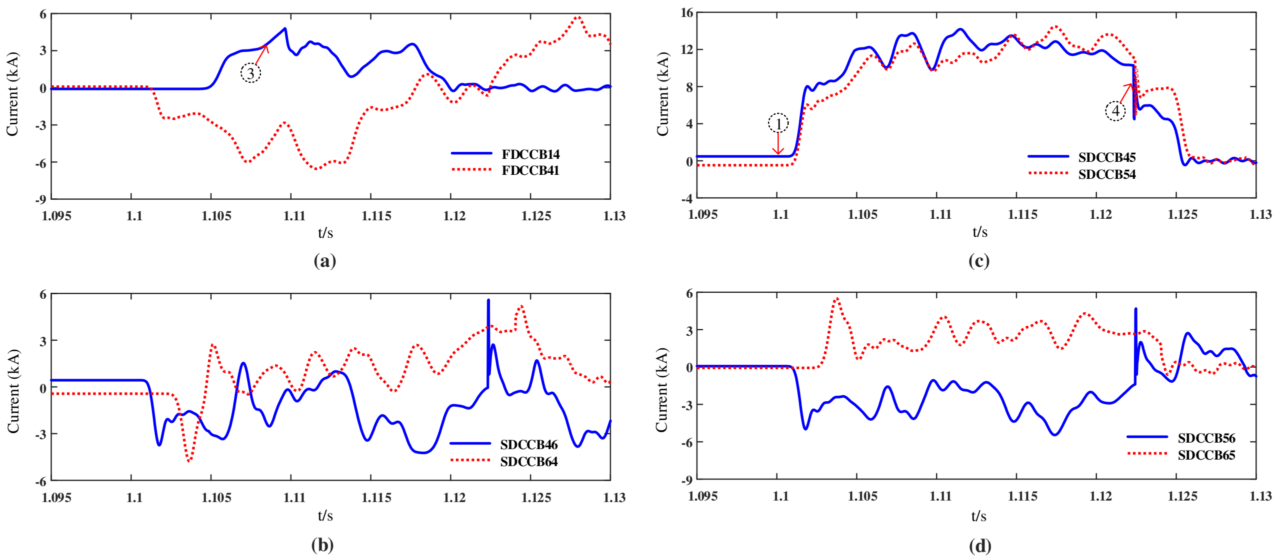

Fig. 7. System behaviour during fault isolation and restoration processes after a fault event in Zone 1 at 1.1s
(a) DC currents flowing through DC circuit breakers FDCCB14 and FDCCB41, (b) DC currents flowing through DC circuit breakers SDCCB46 and SDCCB64, (c) DC currents flowing through DC circuit breakers SDCCB45 and SDCCB54, (d) DC currents flowing through DC circuit breakers SDCCB56 and SDCCB65

Upon the opening of all relevant DCCBs, the DC currents and the active power in Station 4-6 are quickly brought to zero (see Fig.6 (d) and Fig.7). On the other hand, the isolation of the faulty cable in Zone 1 results in the recovery of the DC voltage (initially through the diodes in the converter stations) and oscillations are observed in Fig.6(b) for Station 4-6 around 1.12-1.15s.

5.3. System Restoration

In Table 2, stages 5-8 indicate system recovery. After the faulty cable C45 is disconnected by opening the relevant mechanical DCCBs, Station 4-6 are re-enabled at 1.159s, 1.161s and 1.160s respectively (55ms after their blocking, see stage 5 in Table 2) and are all set to operate at DC voltage control mode initially. Once the voltage of DC cable C56 reaches the predefined value of 760 kV SDCCB65 is reclosed at 1.274s (stage 6). Then all the stations in Zone 1 are restored to their pre-fault control modes where Station 4 and 6 start exchanging power within Zone 1 at 1.4s (stage 7) with a ramp of 3000MW/s. The fast-acting DCCBs are reclosed at 1.51s (stage 8) to reconnect Zone 1 and 2. In this simulation study, the system reaches steady state within 200-300ms after the recovery process.

6. Conclusion

This paper proposes a DC fault protection arrangement and system recovery strategy of large partitioned MTDC networks. Fast acting DCCBs are installed at strategic locations to allow quicker fault isolation in case of a fault event in one of the DC network zones where protection inside each DC zone is achieved using slow DCCBs or ACCBs with DC switches. This proposed protection configuration ensures accurate and robust protection option for the system with low investment in protection cost, and continuous operation of the healthy zones during a fault event in the MTDC network to limit the maximum ‘loss-of-main’ to the connected AC networks. The simulation results of a two-zone six-terminal MTDC network with radial and meshed configurations confirm the viability of the protection arrangement and system recovery strategy. The proposed system restoration approach gives a smoother restart of the faulty zone as well as reduce unwanted voltage overshoot and oscillation significantly and reduces the transients when the relevant DCCBs/DCSs are reclosed. The proposed DC network partition, fault protection arrangement and system recovery strategy concept provide a design option for future larger MTDC networks which has low investment in protection cost and limited ‘loss-of-infeed’ to connected AC networks.

7. References

[1] L. Tang and B.-T. Ooi, "Locating and Isolating DC Faults in Multi-Terminal DC Systems," IEEE Trans. on Power Delivery, vol. 22, pp. 1877-1884, 2007.

[2] R. Li, L. Xu, D. Holliday, F. Page, S. Finney, and B. Williams, "Continuous Operation of Radial Multi-terminal HVDC Systems under DC Fault," Power Delivery, IEEE Transactions on, vol. PP, pp. 1-1, 2015.

[3] M. Hajian, L. Zhang, and D. Jovcic, "DC Transmission Grid With Low-Speed Protection Using Mechanical DC Circuit Breakers," IEEE Trans. Power Del., vol. 30, pp. 1383-1391, Jun. 2015.

[4] M. H. Rahman, L. Xu, and L. Yao, "Protection of large partitioned MTDC Networks Using DC-DC converters and circuit breakers," Protection and Control of Modern Power Systems, vol. 1, p. 19, 2016.

[5] C. MacIver, K. R. W. Bell, and D. P. Nedic, "A Reliability Evaluation of Offshore HVDC Grid Configuration Options," Power Delivery, IEEE Transactions on, vol. PP, pp. 1-1, 2015.

[6] K. Tahata, S. El Oukaili, K. Kamei, D. Yoshida, Y. Kono, R. Yamamoto, et al., "HVDC circuit breakers for HVDC grid applications," in AC and DC Power Transmission, 11th IET International Conference on, 2015, pp. 1-9.

[7] M. Callavik, A. Blomberg, J. Hafner, and B. Jacobson, "The hybrid HVDC breaker: An innovation breakthrough enabling reliable HVDC grids," ABB Grid Systems, Tech. Rep.,Nov. 2012.

[8] L. Rui and X. Lie, "Review of DC fault protection for HVDC grids," Wiley Interdisciplinary Reviews: Water, 10/6 2017.

[9] R. Marquardt, "Modular Multilevel Converter topologies with DC-Short circuit current limitation," in Power Electronics and ECCE Asia (ICPE & ECCE), 2011 IEEE 8th International Conference on, 2011, pp. 1425-1431.

[10] R. Zeng, L. Xu, L. Yao, and B. W. Williams, "Design and Operation of a Hybrid Modular Multilevel Converter," IEEE Trans. on Power Electronics vol. 30, pp. 1137-1146, 2015.

[11] Ofgem, "National Electricity Transmission System Security and Quality of Supply Standard (NETS SQSS): Review of Infeed Losses (GSR007 as revised by GSR007-1)," ReportJan. 2011.

[12] M. H. Rahman, L. Xu, and Y. Liangzhong, "DC fault protection strategy considering DC network partition," in 2016 IEEE Power and Energy Society General Meeting (PESGM), 2016, pp. 1-5.

[13] J. Peralta, H. Saad, S. Dennetiere, J. Mahseredjian, and S. Nguefeu, "Detailed and Averaged Models for a 401-Level MMC HVDC System," IEEE Trans. Power Del., vol. 27, pp. 1501-1508, Apr. 2012.

[14] E. Kontos, R. T. Pinto, S. Rodrigues, and P. Bauer, "Impact of HVDC Transmission System Topology on Multiterminal DC Network Faults," IEEE Trans. on Power Delivery, vol. PP, pp. 1-1, 2014.

[15] T. Eriksson, M. Backman, and S. Halen, "A low loss mechanical HVDC breaker for HVDC Grid applications," in Proc. Cigré Session,, Paris, France, 2014.

[16] E. Kontos, R. T. Pinto, and P. Bauer, "Fast DC fault recovery technique for H-bridge MMC-based HVDC networks," in 2015 IEEE Energy Conversion Congress and Exposition (ECCE), 2015, pp. 3351-3358.

[17] C. Chen, G. P. Adam, S. Finney, J. Fletcher, and B. Williams, "H-bridge modular multi-level converter: control strategy for improved DC fault ride-through capability without converter blocking," IET Power Electronics, vol. 8, pp. 1996-2008, 2015.